NATURE MATERIALS DOI: 10.1038/NMAT2592

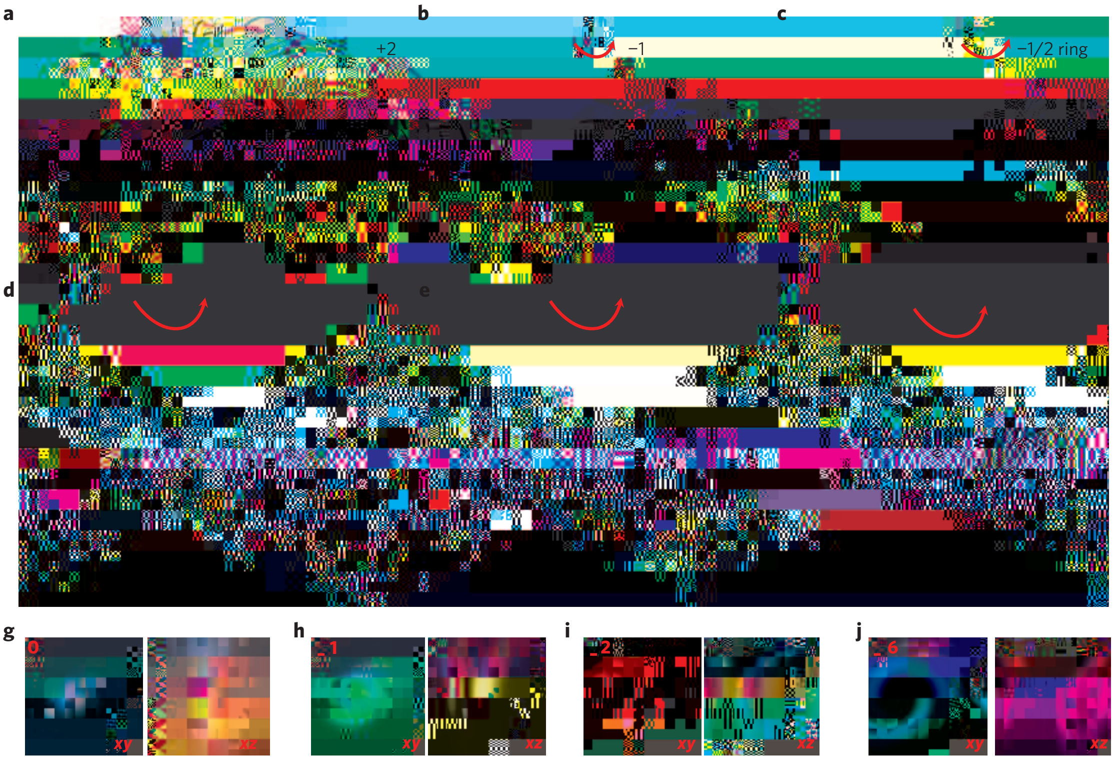

Figure 1 | T3 field configurations generated by Laguerre–Gaussian beams and embedded into a uniform field by defects. **a**, Toron structure with the topological charge '+2' owing to the twist-escaped non-singular disclination ring of strength $s = +1$ shown by the red line. **b**,**c**, '−1' hyperbolic point defect (**b**) and a ring of $s = -1/2$ disclination topologically equivalent to a '−1' point defect (**c**), both showing twist of $\hat{n}(\mathbf{r})$ with the sense of twist shown by the red arrows. **d**, T3-1 configuration with the toron accompanied by two hyperbolic point defects. **e**, T3-2 structure containing a point defect and a disclination ring. **f**, T3-3 configuration with two $s = -1/2$ defect rings. **g**–**j**, Light-intensity distributions in the lateral *xy* (left) and axial *xz* (right) planes of the Laguerre–Gaussian beams of topological charge marked for each of the image pairs; the square cross-sections are 4 µm wide.

structures remain to be explored. The CNLCs studied here have helicoidal ground-state director structure and are of special interest from this standpoint. In our experiments, the beams of charge $l = 0 - \pm 10$ and intensity distributions in the lateral and axial

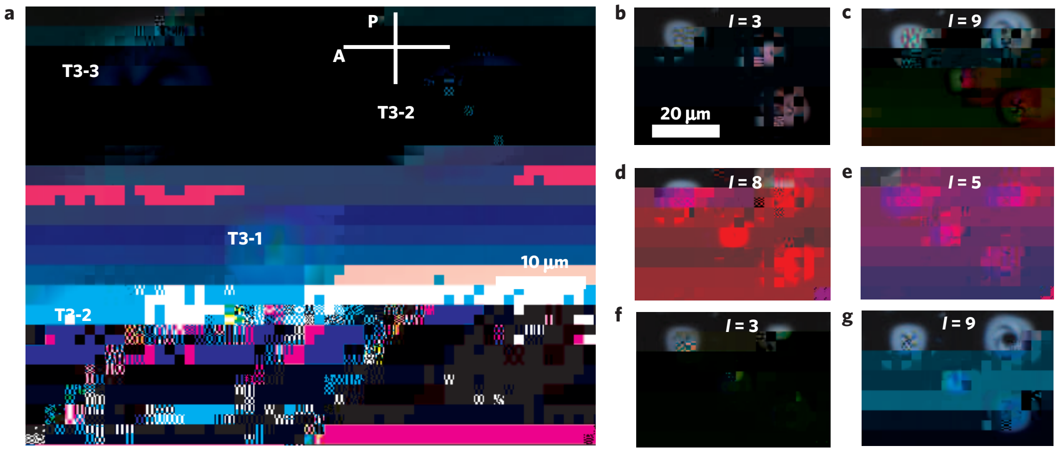

Figure 2 | Predetermined optical generation and switching of the toron structures. a, Polarizing optical microscopy texture showing T3-1 (the smallest), two T3-2s of opposite winding (intermediate size) and T3-3 (the largest structure) generated next to each other. The inset shows the letters 'CU' obtained by optical generation of four T3-2s per letter at the letters' vertices and T3-1 elsewhere within the characters. The orientations of the crossed polarizer (P) and analyser (A) are shown by the white bars. **b**

Table 1 | Material parameters of the used nematic hosts and chiral additives.

Material/property	K_{11} (pN)	K_{22} (pN)	K_{33} (pN)	$\Delta\varepsilon_{lf}$	Δn	H_{HTP} of CB-15 (μm^{-1})	H_{HTP} of S-811 (μm^{-1})
MLC-6609	17.2	7.51	17.9	−3.7	0.078	-	−10.5
ZLI-3412	14.1	6.7	15.5	+3.4	0.078	+6.3	−8.8
MLC-6815	-	-	-	+8.1	0.052	+6.5	−10.7

example, the letters 'CU' in the inset of Fig. 2a are composed of T3-2s at the corners and T3-1s elsewhere within the characters. Generation of different T3s depends on the initial laser-induced director tilt from the vertical alignment, which, in turn, depends on the intensity distributions shown in Fig. 1g–j. Beams having large $|l|$ with high-intensity lobes in the axial plane pointing outward from the low-intensity centre generate T3-2s or T3-3s, whereas the beams with small $|l|$ generate T3-1s. For example, in a cell with $p \approx d = 5\,\mu m$, the T3-1 structure is induced by the Laguerre–Gaussian beams of $l = \pm(0-4)$, the T3-2 is observed for $l = \pm(4-8)$ and T3-3 is observed for $|l| > 8$. Therefore, T3s can be reversibly transformed between each other as shown in the top right corner of Fig. 2c–g. The threshold generating laser powers are comparable for all T3s and vary from 60 mW for $l =$


Splay

DOI: 10.1038/NMAT2592

$-$+/)*+!1*$-7&!01!:,2%$))$>A,%&&*,'!4$,(&!/5,/!5,?$!/0)%&>-*F$!*'/$'&*/3!7*&/)*4%/*0'&!GS*2;!"2>QJ!,'7!/5,/!*'7%+$!/0)0*7>&5,=$7!*'*/*,-!7$10)(,/*0'&!01!/5$!7*)$+/0)!1*$-7!7$=$'7*'2!0'!/5$!+5,)2$!/!,'7!),7*%&!)!01!/5$!?0)/$C!4$,(!*'!*/&!-,/$),-!=-,'$;!Z'!,2)$$($'/!B*/5!$C=$)*($'/&D!/5$!*'*/*,-!-0+,/*0'!01!/5$!4$,(]&!10+,-!=-,'$!,+)0&&!/5$!&,(=-$]&!/5*+F'$&&!70$&!'0/!5,?$!,!&*2'*1*+,'/!$11$+/!0'!/5$!&=,/*,-!-0+,/*0'!01!/5$!2$'$),/$7!<0)0';!T-/50%25!(0&/!01!/5$!'%($)*+,-!)$&%-/&!/5,/!B$!=)$&$'/!*'!/5*&!B0)F!5,?$!4$$'!04/,*'$7!10) / p = 1

DOI: 10.1038/NMAT2592

→ (, ,)

,

 DOI: 10.1038/NMAT2592

!

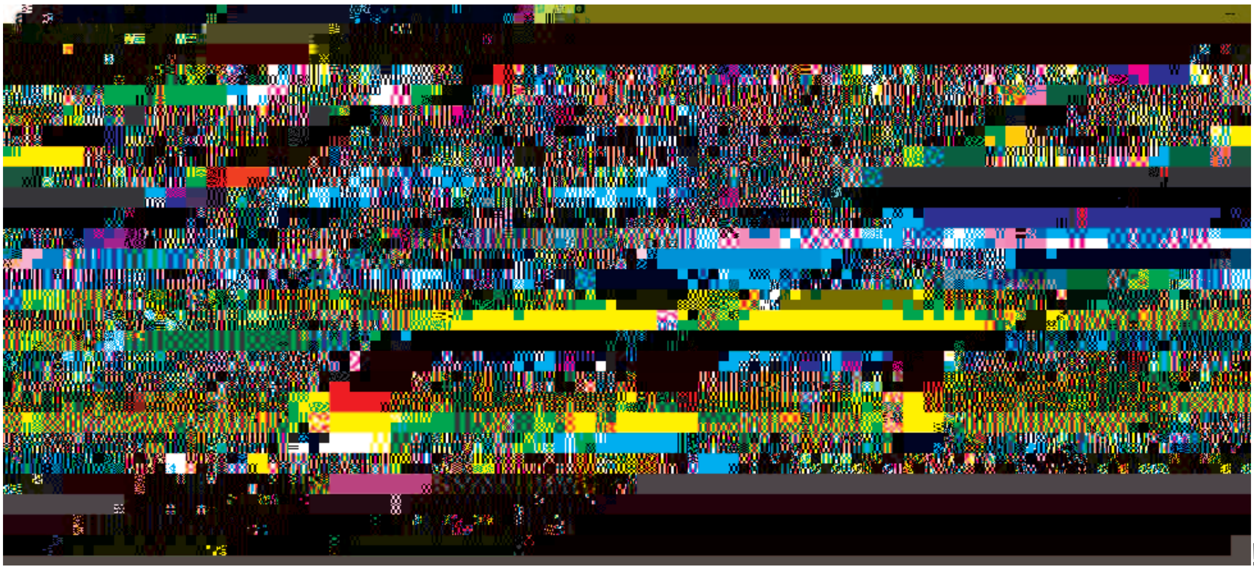

!

08 4=12, ! N/, I ; J ?=:21M<8 J =@6:27, Q21:896@, 91 ; <<M<29:8 ; 3<, ; K, :L2, (NM . , <:1=9:=12/, , 6G! <5$! &/)%+/%)$! +0 ' &*&/&! 01! /5$!) , 7*, -! /B*&/! 01! $\hat{n}(\vec{r})$ *' ! /5$! +$ ' /) , -! =-, ' $! 01! /5$! +$--! , &! B$--! , &! /B0! =0* ' /! 7$1$+/&! +-0&$! /0! /5$! &%4&/) , /$&j! /5$! * ' &$/&! &50B! &* (%-, /$7! $\hat{}(\vec{r})$